# Efficient Production of Human beta-Defensin 2 (HBD2) in Escherichia coli

**Post-print of a peer-reviewed article published by Bentham Science Publishers.**
**Final published article available at: http://dx.doi.org/10.2174/092986609788490122**

**Cite as:**
**Vargues, T., Morrison, G. J., Seo, E. S., Clarke, D. J., Fielder, H. L., Bennani, J., Pathania, U., Kilanowski, F., Dorin, J. R., Govan, J. R. W., Mackay, C. L., Uhrin, D., & Campopiano, D. J. (2009). Efficient Production of Human beta-Defensin 2 (HBD2) in Escherichia coli. Protein and Peptide Letters, 16(6), 668-676.**

**Manuscript received: 11/02/2008; Accepted: 23/10/2008; Article published: XX/06/2009**

# Efficient production of human β-defensin 2 (HBD2) in *Escherichia coli***

Thomas Vargues,[1,#] Gareth J. Morrison,[1,#] Emily S. Seo,[1] David J. Clarke,[1] Helen L. Fielder,[1] Julien Bennani,[1] Uday Pathania,[2] Fiona Kilanowski,[2] Julia R. Dorin,[2] John R. W. Govan,[3] Logan Mackay,[1] Dušan Uhrín[1] and Dominic J. Campopiano[1,*]

[1]EaStCHEM, School of Chemistry, Joseph Black Building, University of Edinburgh, West Mains Road, Edinburgh, EH9 3JJ, UK.

[2]Medical Research Council Human Genetics Unit, Edinburgh, EH4 2XU, Scotland, UK.

[3]Centre for Infectious Diseases, University of Edinburgh, Edinburgh EH16 4SB, UK.

[*]Corresponding author; e-mail: Dominic.Campopiano@ed.ac.uk, tel.: + 44 131 650 4712, fax: + 44 131 650 4743

[**]This work was supported by awards from the Biotechnology and Biological Sciences Research Council (BBSRC), the Engineering and Physical Sciences Research Council (EPSRC), the Cystic Fibrosis Trust, the University of Edinburgh, the Medical Research Council UK (MRC), Scottish Enterprise and the Royal Society of Edinburgh. We thank members of the RASOR Mass Spectrometry facility and Doctoral Training Centre and Team Defensin for help and advice.

[#]These authors contributed equally to this work.

**Keywords:**
HBD2, defensin, peptide, E. coli, chemotaxis, antimicrobial activity.

**Abstract**

Human β-defensin 2 (HBD2) has been shown to interact with pathogenic bacteria and components of the mammalian innate and adaptive immune response. We describe a quick and reliable method for the production of HBD2 in *Escherichia coli.* HBD2 was expressed as an insoluble fusion, chemically cleaved and oxidised to give a single, folded HBD2 β-isoform. The purified peptide was analysed by high resolution mass spectrometry, displayed a well-dispersed $^{1}$H NMR spectrum, was a chemoattractant to HEK293 cells expressing CCR6 and acted as an antimicrobial agent against *E. coli, P. aeruginosa* and *C. albicans*.

**Introduction**

Antimicrobial peptides (AMPs) are essential components of the innate immune response and act as the first line of defence against invading pathogens [1]. The AMP family displays enormous sequence, structural and functional diversity and over 900 different eukaryotic peptides have been characterized to date (sequences are available in the Antimicrobial Sequences Database (AMSDb), http://www.bbcm.univ.trieste.it/). Defensins are a subset of the AMP family and are small (3-5 kDa), cationic peptides that play roles in both innate and adaptive immunity [2-7]. They are characterised by 6 conserved cysteine residues that form 3 disulfide bonds and are divided into two main subfamilies; alpha (α-) and beta (β-) are defined by their cysteine spacing, disulfide bond connectivity and genomic organisation. The α-defensins display $Cys_1$–$Cys_6$, $Cys_2$-$Cys_4$, $Cys_3$-$Cys_5$ S-S connectivity and contain ~29-35 residues, whereas the β-defensins display a S-S connectivity of $Cys_1$-$Cys_5$, $Cys_2$-$Cys_4$, $Cys_3$-$Cys_6$ and consist of ~40-50 residues. A third subfamily, the θ-defensins also contain 3 S-S bonds but are cyclic peptides, fused at the N- and C-termini, and have only been found in rhesus monkeys.

Analysis of the human genome revealed the presence of considerably more β-defensin genes than previously thought [8]. In contrast, only 6 human α-defensins have been identified [9] and elegant studies of the structures and properties of these peptides (HNP1-4 and HD5 and HD6) by a number of research groups have begun to provide a better understanding of their role in the immune response [7,10-14]. The high resolution structures of a few of the known mammalian β-defensins have been determined by NMR spectroscopy and x-ray crystallography and include bovine neutrophil BD-12, penguin spheniscin and the human β-defensins (HBD1, HBD2, HBD3) [15-22], but more work is needed to explore the structure/functional relationship of this sub-family. We have chosen HBD2 as a target; it was shown that this defensin is expressed in epithelial cells and in the epidermis, and was originally isolated from human psoriatic scales [23]. It is expressed as a 64 amino acid precursor peptide and the mature form consists of 41 residues with a net positive charge of +7. The 3D structure of mature HBD2 revealed an amphipathic molecule with distinct patches of positively-charged and hydrophobic residues [17,19,20]. It is thought that this topology allows the defensin to interact with the outer cell components of bacterial membranes and act as a potent antimicrobial peptide against a range of pathogens [24].

Recent studies have shown that a number of defensins and their related peptide fragments, can act also as potent stimulators of the adaptive immune response, e.g. HBD2 acts as a chemoattractant for CD4 memory T cells and immature (but not mature) dendritic cells, by acting through the chemokine receptor CCR6, a member of the G-protein coupled receptor (GPCR) family [25,26].

To study the molecular details of the interaction of HBD2 with its various targets we required a robust method for the production of single isoform material. The production of defensins suitable for structural and functional studies has been achieved by solid-phase peptide synthesis but the inherent amphiphilic nature of the peptide, protection strategies and losses upon oxidation have caused associated problems [27,28]. As an alternative, recombinant methods have also been developed, e.g., Ganz and colleagues have used a baculovirus/insect cell system to produce active human peptides HNP-1, HD-5, HBD1 HBD2 [29-32]. As well as this method others have employed the common, easy-to-use host *E. coli* [33-36]. Here however, there is the inevitable problem of toxicity of the defensins towards the host expression system but this has been overcome by expressing the peptide fused to a protein partner within inclusion bodies. This introduces a further cleavage step to release the mature peptide and results in low overall yield. The use of expensive proteases such as enterokinase also increases the cost of the overall production of sufficient quantities of peptide. New strategies such as using the yeast *Saccharomyces cerevisiae* as a host organism or production by a cell-free system have also emerged recently [37,38]. These combined methods have allowed researchers to begin to explore the structure and activity of certain defensins [22,39-42].

To produce defensins for a range of structural and functional studies, we describe a method for the production of recombinant, active, single isoform β-HBD2 from an *Escherichia coli* host. We designed a codon-optimised HBD2 gene for bacterial expression and synthesised this gene by recursive PCR [43] (Figure 1). and developed a protocol to isolate mature HBD2. This peptide was characterised by a range of structural techniques and was active in functional assays.

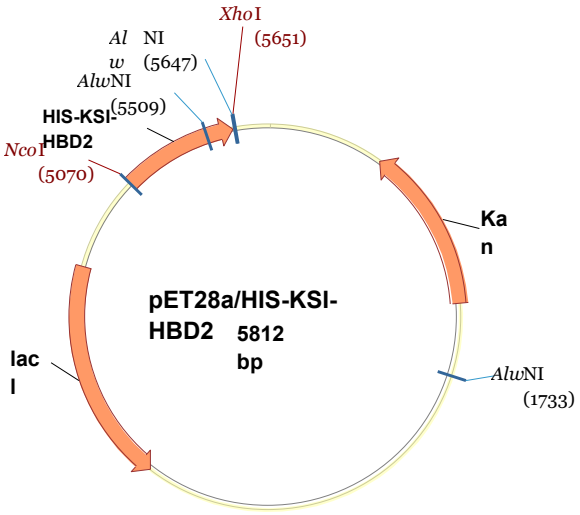


(A)

***AlwNI*** MetGlyIleGlyAspProValThrCysLeuLysSerGlyAlaIleCysHis

**1 CAGGCGCTG**ATGGGTATCGGTGACCCGGTTACCTGCCTGAAATCCGGTGCTATCTGCCAC 60

**GTCCGCGAC**TACCCATAGCCACTGGGCCAATGGACGGACTTTAGGCCACGATAGACGGTG

ProValPheCysProArgArgTyrLysGlnIleGlyThrCysGlyLeuProGlyThrLys

**61** CCGGTTTTCTGTCCGCGTCGTTACAAACAGATCGGTACCTGCGGTCTGCCGGGTACCAAA 120

GGCCAAAAGACAGGCGCAGCAATGTTTGTCTAGCCATGGACGCCAGACGGCCCATGGTTT

CysCysLysLysPro*** ***AlwNI***

**121** TGCTGCAAAAAACCGTGA**CAGATGCTG 147**

ACGACGTTTTTTGGCACT**GTCTACGAC**

(B)

1 MGSSHHHHHH SSGLVPRGSH AHTPEHITAV VQRFVAALNA GDLDGIVALF

51 ADDATVEDPV GSEPRSGTAA IREFYANSLK LPLAVELTQE VRAVANEAAF

101 AFTVSFEYQG RKTVVAPIDH FRFNGAGKVV SIRALFGEKN IHACQALM**GI**

151 **GDPVTCLKSG AICHPVFCPR RYKQIGTCGL PGTKCCKKP**

(C)

***Figure 1.*** **A.** Schematic representation of expression vector pET-28a/HIS-KSI-HBD2. **B.** Design of synthetic, codon-optimized HBD2 gene (147 bp) for *E. coli* expression. Primers were designed for overlapping recursive PCR (see Table 1). The 5' and 3' primers incorporated *Alw*N1 restriction sites (bold) to allow cloning of KSI-HBD2 fusion into pET28a. **C.** The full-length His-KSI-HBD2 fusion sequence (189 aa) with mature HBD2 (41 aa) produced by CNBr cleavage after the Met residue highlighted in bold. The Met-Ala mutations in KSI (M1A and Met126A) are underlined.

## Materials and methods

### *Materials*

*E. coli* strains Top10 (Invitrogen) and BL21 (DE3) (Novagen) were used for construction of plasmids and expression of proteins respectively. Polymerase chain reaction (PCR) was carried out using Hercules polymerase (Stratagene) and puRe Taq Ready-To-Go PCR beads (GE Healthcare). PCR products were cloned initially in pGEM-T easy (Promega), then re-cloned into pET plasmids (Novagen). Site-directed mutagenesis used the Quick-change kit (Stratagene). Nickel-nitrilotriacetic acid (Ni-NTA) affinity resin was from Qiagen. Snakeskin dialysis tubing was from Pierce (3 kDa cut-off). Oligonucleotide primers were purchased from SigmaGenosys. All restriction enzymes and T4 DNA ligase were from New England Biolabs. Nu-PAGE 12% Bis-Tris pre-cast gels were from Invitrogen. HPLC columns were purchased from Phenomenex, synthetic human β-defensin 2 (bHBD2, biotinylated at the N-terminus) was purchased from Albachem and Polymyxin B (PMB) was obtained from Calbiochem and tris(2-carboxyethyl)phosphine (TCEP) and CNBr were from Sigma.

### *Synthesis and cloning of codon-optimized HBD2*

Six overlapping primers (Table 1) with codons optimized for expression in *E. coli* were designed using the mature HBD2 amino acid sequence (also known as DEFB4, Genbank accession number, NM_004942). The reaction contained in a final volume of 100 µl: 10 µl (100 pmol) of the outermost 5' primers (P1 and P6) of each strand, 10 µl (10 pmol) of the internal primers (P2 – P5), 4 µl DMSO, 10 µl 10 x Herculase reaction buffer (Stratagene), 1 µl Herculase Hotstart DNA polymerase (Stratagene), 4 µl 25 mM dNTPs, 21 µl $dH_2O$ and was subjected to 30 PCR cycles of 95 ºC for 2 minutes, 40 ºC for 3 minutes and 72 ºC for 30 seconds. A second amplification was performed to confirm annealing of all six primers in a final volume of 50 µl: 5 µl primer P1 (50 pmol), 5 µl primer P6 (50 pmol), 2 µl template, 38 µl $dH_2O$ and 2 puRe Taq Ready-To-Go PCR beads were subjected to 30 PCR cycles of 95 ºC for 2 minutes, 40 ºC for 3 minutes, 72 ºC for 30 seconds and a final extension of 72 ºC for 10 minutes to add A overhangs. The PCR product (Figure 2A) containing the codon-optimized gene preceded by Met and flanking *Alw*N1 recognition sites was purified, cloned into pGEM-T Easy plasmid and a positive clone sequenced to confirm the fidelity of the insert. The target gene was then cut and ligated into the expression plasmid pET-31b (Novagen) to give pET-31b/HBD2. To incorporate a N-terminal His(6)-tag sequence, both pET-31b/HBD2 and pET-28a(+) vectors were cleaved by restriction enzymes *Nde*I and *Xho*I and the HBD2 fragment now containing the ketosteroid isomerase (KSI)-fused gene was cloned into pET-28a (Figure 1A). To avoid CNBr cleavage at unwanted sites within the fusion residues Met 1 and 126 of KSI were replaced with Ala by site-directed mutagenesis to give plasmid pET-28a/His-KSI-HBD2 (Figure 1 C). The fidelity of this clone was confirmed by DNA sequencing.

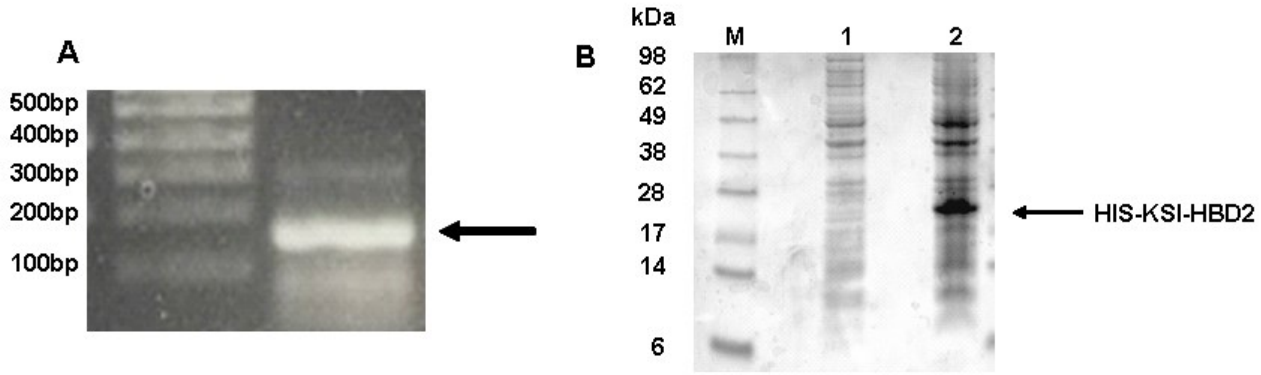


***Figure 2.*** **A.** Synthesis of optimised HBD2 gene by recursive PCR. Lane 1, 1kb DNA Hyperladder I (Bioline); lane 2, recursive HBD2 PCR product. The band indicated by arrow is the 147bp codon-optimised HBD2 gene product. **B**. Expression of HIS-KSI-HBD2 in pET-28/HisKSI. 12 % Bis-Tris acrylamide gel analysis before and after induction with IPTG. Lane M, SeeBlue 2 protein marker (Invitrogen); lane 1, total bacterial lysate before induction; lane 2 insoluble fraction after induction (His-KSI-HBD2, Mr 20.2 kDa).

***Table 1.*** Primers used in synthesis of codon-optimised HBD2

| Primer | Sequence (5'-3') |
|---|---|
| P1 | CAGATGCTGATGGGTATCGGTGACCCGGTTACCTGCCTGAAATCC |
| P2 | CGGACAGAAAACCGGGTGGCAGATAGCACCGGATTTCAGGCAGGT |
| P3 | CCGGTTTTCTGTCCGCGTCGTTACAAACAGATCGGTACCTGCGGT |
| P4 | GCAGCATTTGGTACCCGGCAGACCGCAGGTACCGAT |
| P5 | ACCAAATGCTGCAAAAAATGACAGATGCTG |
| P6 | CAGCATCTGTCACGGTTTTTTGCAGCATTTGGTACCCGG |
| M1A For | GCGGCAGCCATGCGCATACCCCAGAACACATC |
| M1A Rev | GATGTGTTCTGGGGTATGCGCATGGCTGCCGC |
| M126A For | GAATATTCACGCATGCCAGGCGCTGATGGGTATCGGTGAC |
| M126A Rev | GTCACCGATACCCATCAGCGCCTGGCATGCGTGAATATTC |

***Expression of KSI-HBD2 in E. coli***

The freshly transformed BL21 (DE3) colony containing the pET-28a/His-KSI-HBD2 plasmid was used to inoculate 250 mL of 2YT medium at 37 ºC, with shaking containing 30 μg/mL kanamycin. This was grown for 12 hours and then added to 3 litres of 2YT, containing 30 μg/mL kanamycin to give an $OD_{600}$ 0.1 and divided into six one litre flasks, with approximately 500 mL in each flask. Cells were grown at 37 ºC until an $OD_{600}$ = 0.5, induced with a final concentration of 1 mM isopropyl-β-D-1-thiogalactopyranoside (IPTG), and incubated for a further 6 h. Cells were subsequently harvested by centrifugation (6000 rpm for 10 minutes, 4 °C).

***Isolation of KSI-HBD2 inclusion bodies and production of HBD2***

All centrifugation steps were carried out for 20 minutes at 11000 rpm and 4 ºC. The cell pellet containing highly expressed HisKSI-HBD2 was suspended in 5 mL/g in resuspension buffer (50 mM Tris, 25% sucrose, 1 mM EDTA, 0.1% sodium azide, 10 mM DTT, pH 8.0), before addition of 50 mg/mL lysozyme, 500 mM $MgCl_2$ and 10µl DNase. After incubation for 30 minutes at room temperature, lysis buffer (50 mM Tris, 1% Triton X-100, 100 mM NaCl, 0.1% sodium azide, 10 mM DTT, pH 8.0) was added (5 mL/g wet weight original pellet) and incubated for 45 minutes at room temperature. To this cloudy suspension, EDTA (500 mM) was added to give a final concentration of 1 mM, and the sample was snap-frozen in liquid $N_2$ before immediately thawing for 30 minutes in a 37 ºC water bath. To this thawed extract, $MgCl_2$ (500 mM) was added to give a 1mM final concentration and the sample was incubated at room temperature for 1 h to allow the viscosity to decrease before centrifugation. The supernatant was discarded and the pellet from this step was resuspended in an appropriate volume of buffer (50 mM Tris, 1% Triton X-100, 100 mM NaCl, 1 mM EDTA, 0.1% NaAzide, 1 mM DTT, pH 8.0), sonicated for 4 x 30 second blasts and centrifuged. The resulting pellet was then washed in 1 M Guanidine HCl buffer (1 M GuHCl, 50 mM Tris, 1% Triton X-100, 100 mM NaCl, 1 mM EDTA, 0.1% sodium azide, 1 mM DTT, pH 8.0), sonicated with 4 x 30 second bursts and centrifuged. The resulting pellet (inclusion bodies containing highly enriched KSI-HBD2) was resuspended in ~ 50ml 6 M GuHCl binding buffer (6 M GuHCl, 50 mM Tris, 10 mM imidazole, 500 mM NaCl, 5 mM β-mercaptoethanol, pH 8.0). These inclusion bodies were added to 10 ml pre-equilibrated nickel-nitrilotriacetic acid (Ni-NTA, Qiagen) agarose affinity resin, mixed by rotation for 1 h at 4 $^{o}$C, then decanted into an empty 25 ml column reservoir. The packed resin was washed with 6 M GuHCl binding buffer (50 ml) and then eluted with 25 ml of elution buffer (6 M GuHCl, 50 mM Tris, 120 mM imidazole, 500 mM NaCl, 5 mM β-mercaptoethanol, pH 8.0). This elution step with 120 mM imidazole was then repeated to give 50 ml of purified HisKSI-HBD2. The eluted fusion protein was dialyzed against 25 mM Tris buffer, pH 8.0 overnight at 4 $^{o}$C which caused precipitation of the fusion protein.

The fusion was recovered by centrifugation and the pellet was resuspended in 6 M GuHCl, 25 mM Tris buffer, pH 8.0. To this HCl (5 M stock) was added until the pH was ~1.0. Solid CNBr was added to give a final concentration of 250 mM and cleavage was allowed to proceed for 24 h in the absence of light and under nitrogen. The cleaved mixture was evaporated at 42 $^{o}$C using a rotary evaporator to remove any unreacted CNBr, and the concentrated sample was dialyzed against 25 mM Tris buffer, pH 8.0 overnight at 4 $^{o}$C to cause precipitation of the KSI. The precipitate was removed by centrifugation and the supernatant containing HBD2 was filtered (0. 45 µM) and purified
by RP-HPLC as described below.

***Purification of HBD2***

Preparative RP-HPLC on a Jupiter™ Proteo column was performed with a Waters 600 control pump fitted with a photodiode array 996 detector using Millenium 32 software. The HBD2 isolated from the CNBr cleavage step was applied to the column in 3-4 ml batches, the column was washed with 5% acetonitrile then a linear gradient of 5-55% acetonitrile over 50 minutes at a flow rate of 3 mL/minute was used to elute the HBD2. Fractions were analysed by SDS-PAGE and those containing HBD2 were pooled and shown to be a mixture of partially reduced and oxidized peptides (by ESI-mass spectrometry).

***Oxidation of recombinant HBD2***

The HBD2 recovered by prep-HPLC was freeze-dried then reconstituted in 25 mM Tris, pH 8.0, with 20 mM tris(2-carboxyethyl)phosphine (TCEP) added to convert the peptide to the fully reduced form before re-purification by prep-HPLC using identical conditions as above. Fractions containing HBD2 were freeze-dried then dissolved in 50 mM Tris, pH 8.0, 3 mM cysteine, 0.3 mM cystine and stirred for 4 h at room temperature. The reaction was followed by analytical RP-HPLC and analyzed by ESI-mass spectrometry to confirm that the HBD2 was present in the oxidized form (elution at 40 mins). The final yield of oxidized β-HBD2 is 3-6 mg from 3 litres of *E. coli* culture (based on 10 preparations).

***Western blot analysis***

Peptides were separated on a 12% Bis-Tris gel as described by the manufacturer (Invitrogen) followed by electroblotting using a Trans blot SD Semi-Dry Transfer cell (Bio-Rad) onto a Hybond-ECL nitrocellulose membrane (GE Healthcare). HBD2 was detected with a HBD2-specific antibody (Autogen Bioclear) and electrochemiluminescence plus ($ECL^+$) using a Streptavidin-HRP antibody according to the manufacturer's instructions (GE Healthcare).

***Disulfide bond connectivity***

The disulfide bond connectivity of the oxidized HBD2 was determined by trypsin/chymotrypsin digest, Edman degradation and mass spectrometry analysis as described previously [40,44].

### *1D $^{1}$H NMR Spectrum*

1 mg of oxidized HBD2 was dissolved in 20 mM sodium acetate buffer, pH 4.0 at 25 $^{o}$C and 10% $D_2O$ (v:v) was added to give to a final peptide concentration of 0.46 mM. The $^{1}$H NMR spectrum was recorded on a Bruker AVANCE spectrometer equipped with a cryoprobe operating at 600 MHz and 25 °C. 128 scans were taken with a sweep width of 15 ppm and 8000 complex points. For water suppression double-pulsed gradient spin echo was used.

### *Antimicrobial activity assay*

The purified, oxidized HBD2 was dissolved into 0.01% acetic acid and centrifuged (13000 rpm for 10 minutes, 25 °C) to remove precipitate. The HBD2 was concentrated (Vivaspin 0.5 mL concentrator, 3000 MWCO PES) to 1 mg/mL and stock HBD2 solutions of concentrations 15, 30, 60, 125, 250 and 500 μg/mL were prepared. Antimicrobial assays were carried out according to the method set out in our previous study [25,40,45]. Briefly, a laboratory strain of *E. coli* K-12 MG1655 was grown to midlogarithmic phase (OD at 600nm = 1.0). From this 90 μl *E. coli* (~1.0 x $10^5$ cells) was incubated with 10 μl of each stock HBD2 solution and as a negative control 90 μl *E. coli* was incubated 10 μl 0.01% acetic acid. These samples were incubated at 37 °C for 2 hours. Then 10-fold serial dilutions of the incubation mixture were plated on Iso-Sensitest plates, incubated at 37 °C, and the CFU was determined the following day. Colonies were counted and the $LD_{50}$, $LD_{90}$ (Lethal Dose: amount of peptide required to kill 50 % and 90% of viable cells) and the $MBC_{99.99}$ (Minimum Bactericidal Concentration at 99.99 %) values were calculated from the resulting killing curve. The same antimicrobial assays were performed with *Pseudomonas aeruginosa* (PAO1), a Gram-positive strain *Staphylococcus aureus* (ATCC 25923) and a fungus, *Candida albicans* (J2922) [45]. In parallel, the same strains were used with the antimicrobial agent Polymyxin B (PMB) as a control. All the killing assays were performed at least 3 times for each strain and the values were obtained by taking the mean of each 3 experiments.

### *High resolution FT-ICR mass spectrometry*

The oxidized HBD2 was diluted to a final concentration of 1 μM in electrospray buffer, consisting of 50:50 methanol:$H_2O$ with 0.2 % formic acid. Data was acquired on a 12 Tesla Apex Qe FT-ICR (Bruker Daltonics, Billerica, MA) equipped with mass resolving quadrupole, coupled to a nano-electrospray ionization (nESI) enabled TriVersa Nanomate (Advion Bioscience, Ithaca, NY). Samples were infused at a flow rate of 50 nanolitres per minute. Desolvated ions were transmitted to a 6 cm Infinity cell® penning trap. Trapped ions were excited (frequency chirp 48-500 kHZ at 100 steps of 25 μs) and detected between *m/z* 600 and 2000 for 1 s to yield broadband 1 Mword time-domain data. Each spectrum was the sum of 64 mass analyses. Typical

chamber base pressure was ~9 x $10^{-11}$ mbar. Time-domain FT-ICR data was acquired using an AQS console and the aquisition rate was typically ~1 scan/2 s. Fast Fourier Transforms and subsequent analyses were performed using DataAnalysis (Bruker Daltonics, Billerica, MA).

### *Chemotaxis assay*

The chemotaxis activity analysis was carried out against HEK293 cells expressing CCR6 as we have previously reported [25]. The migration of CCR6-transfected human embryonic kidney HEK293 cells was assessed with a microchemotaxis chamber technique. Chemotactic activity was measured as the optimal concentration of test compound at which the highest chemotactic index value was obtained. Experiments were carried out three times. CCL20 (also known as MIP3-α) was from Peprotech (London, UK).

## Results and discussion

### *Synthesis of HBD2 gene by recursive PCR*

Our goal was to produce mature, untagged HBD2 as a single β-defensin isoform. Our strategy to enhance the expression of the toxic human antimicrobial peptide HBD2 in the host *E. coli* was to fuse it to the highly insoluble ketosteroid isomerase (KSI) tag using a commercially available plasmid. Six overlapping primers (Table 1) with codons optimized for expression in *E. coli* were designed to synthesise the HBD2 gene in a one step recursive PCR reaction [43] (Figure 1B). An ATG Met codon was incorporated at the 5' end of the HBD2 gene to enable cleavage of the peptide from the KSI tag by cyanogen bromide (CNBr) (Figure 1B). A similar chemical cleavage strategy had been used by Ganz and coworkers to produce active HBD2 expressed in baculovirus-infected insect cells [29]. Restriction sites for *Alw*NI, flanking the HBD2 sequence, were engineered into the gene to enable cloning into the KSI expression plasmid, pET-31b and a stop codon was engineered upstream of the 3' *Alw*NI site to avoid generation of a homoserine lactone HBD2 derivative after cleavage. Initial PCR gave a gene product at the expected size of the HBD2 target (144bp, Figure 2A) and a second PCR amplification using this template with the 5' and 3' terminal primers gave a gene that was cloned firstly into plasmid pGem-T Easy then into the expression plasmid pET-31b digested with the same enzyme. To utilize His-tag purification technology, the KSI-HBD2 fusion gene was excised from pET-31b and ligated into pET-28a downstream of a 6xHis-tag. To improve the efficiency of the chemical cleavage and generate a single CNBr cleavage site within the KSI-HBD2 fusion, the Met1 and Met126 residues within the KSI gene were converted to Ala by site-directed mutagenesis to generate the expression plasmid pET-28a/His-KSI-HBD2 which was used for all further studies (Figure 1A).

***Expression of His-KSI-HBD2***

Plasmid pET-28a/His-KSI-HBD2 was used to transform BL21 (DE3) cells and on a small scale (10ml) induction with IPTG, a strong band corresponding to His-KSI-HBD2 at 20.2 kDa was observed by SDS-PAGE in agreement with the predicted molecular weight of the KSI-HBD2 fusion protein of 189aa (Figure 2B). This expression was scaled up to 3 litres of culture medium and yielded ~9 g wet weight cell paste that was frozen at -20 °C.

***Purification of His-KSI-HBD2 and cleavage of HBD2***

The His-KSI-HBD2 fusion was isolated from the bacterial pellet by a series washing and centrifugation steps. Aliquots were removed throughout the purification protocol and analysed by SDS-PAGE to monitor the increased purity and yield of His-KSI-HBD2. We engineered a methionine residue at the N-terminus of the HBD2 protein to allow cleavage from the KSI tag by CNBr. This non-enzymatic cleavage is efficient and less expensive than using proteolytic enzymes such as enterokinase. After a one-step Ni-NTA affinity purification, the His-KSI-HBD2 was sufficiently pure for CNBr cleavage (Figure 3A). After 18-22 h, the cleavage was complete and separation of the fusion protein from HBD2 was carried out by dialysis against buffer (25 mM Tris, pH 8.0) followed by centrifugation (10,000 r.p.m.) to remove any precipitate. Cleaved HBD2 was shown to be in the soluble fraction by SDS-PAGE (Figure 3A).

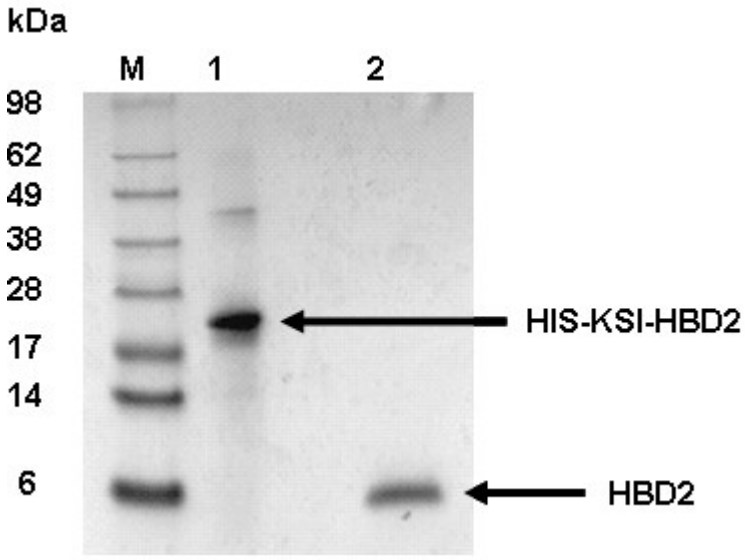


(A)

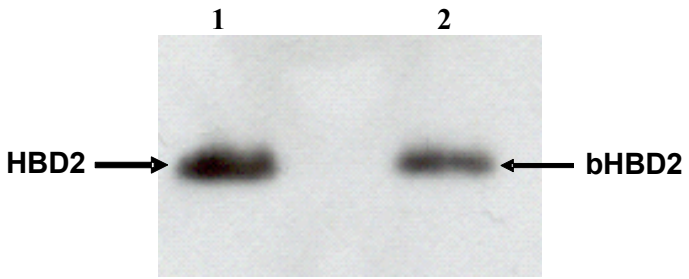


(B)

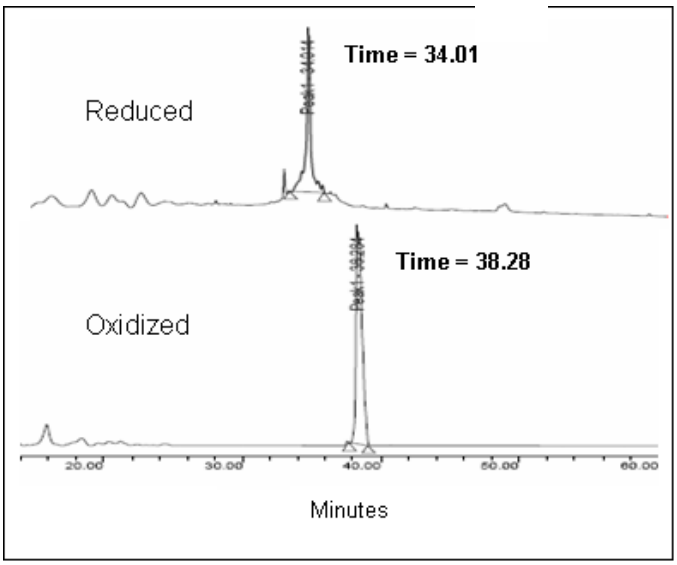


(C)

***Figure 3.*** Purification of recombinant HBD2 **A**. 12 % Bis-Tris acrylamide gel analysis of HIS-KSI-HBD2 fusion (lane 1) and recovered, soluble HBD2 after CNBr cleavage (lane 2) (M, SeeBlue 2 marker (Invitrogen)). **B.** Western blot of oxidized HBD2 probed with anti-HBD2 antibody (Lane 1, Oxidised HBD2 (2.5 μg); lane 2, Synthetic biotinylated bHBD2 (1 μg)). **C**. Reverse-phase HPLC chromatograms of reduced HBD2 (upper trace, ~34 mins) and oxidized HBD2 (lower trace, ~38 mins).

### *Characterisation of oxidized, folded β-defensin HBD2*

Soluble HBD2 was purified by preparative RP-HPLC and mass spectrometry showed that it was a mixture of reduced and oxidized forms. This HBD2 mixture was completely reduced using TCEP then purified by RP-HPLC. The recovered HBD2 was oxidized at room temperature using a cysteine/cystine redox buffer. The fully oxidized form has a longer retention time (~4 minutes) compared to the reduced form (Figure 3C) in agreement with previously published data [44]. This peptide was reactive in a Western blot assay with anti-HBD2 antibody that confirms the identity of the purified HBD2 (Figure 3B). High resolution FT-ICR mass spectrometry was used to determine the accurate mass of HBD2 and confirm its oxidation state. The HBD2

ionized efficiently displaying three charge states (+3, +4 and +5) and the isotopic distribution for the +4 charge state and mass fit to those predicted for fully oxidised HBD2 with an elemental composition ($C_{188}H_{305}N_{55}O_{50}S_6$) and average mass of 4328.23 Da (Figure 4). After purification and freeze drying, ~3-6 mg of fully oxidised β-HBD2 was obtained. The 1D $^1$H NMR spectrum shows sharp, well-dispersed peaks in the amide region, which is indicative of a folded structure (Figure 5). Furthermore, it was important to carry out trypsin/chymotrypsin digest and Edman degradation analysis which showed that the peptide displayed the β-defensin (1-5, 2-4, 3-6) connectivity (data not shown).

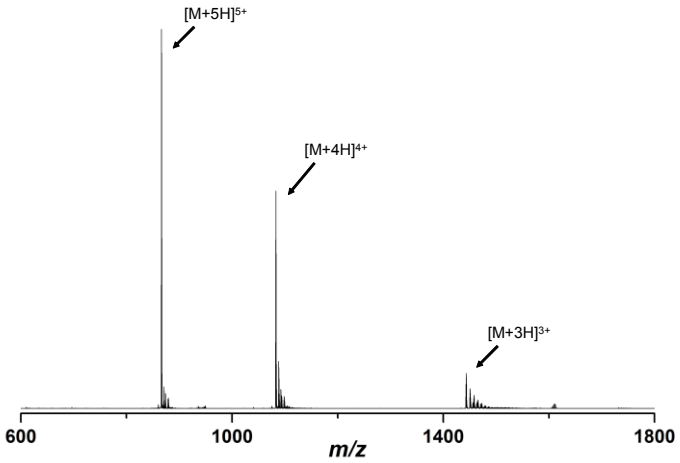


(A)

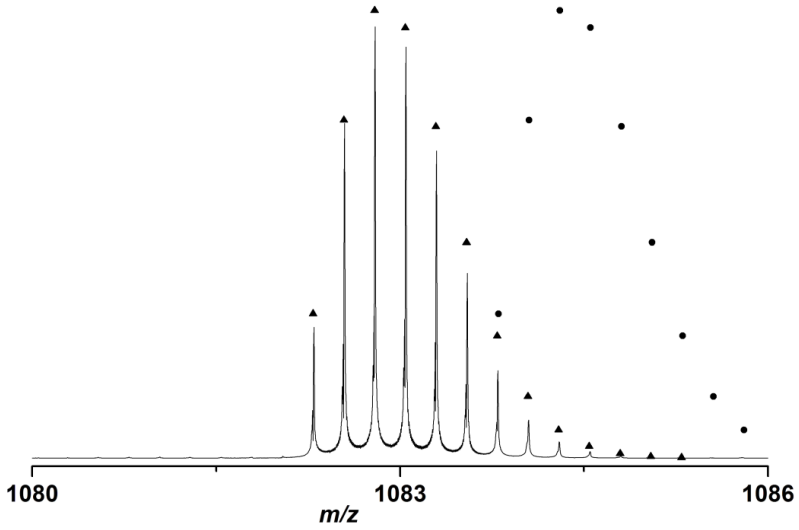


(B)

***Figure 4.*** FT-ICR high resolution mass spectrometry analysis of recombinant HBD2. **A**. The ion envelope for nanospray FT-ICR analysis of oxidized HBD2 showing the +5 to +3 charge states. **B.** The isotopic envelope of the +4 charge state of oxidized HBD2. Closed circles represent the theoretical envelope expected from a

HBD2 monomer with all cysteines reduced and the closed triangles represent that expected from a fully oxidized HBD2 with 3 S-S bonds.

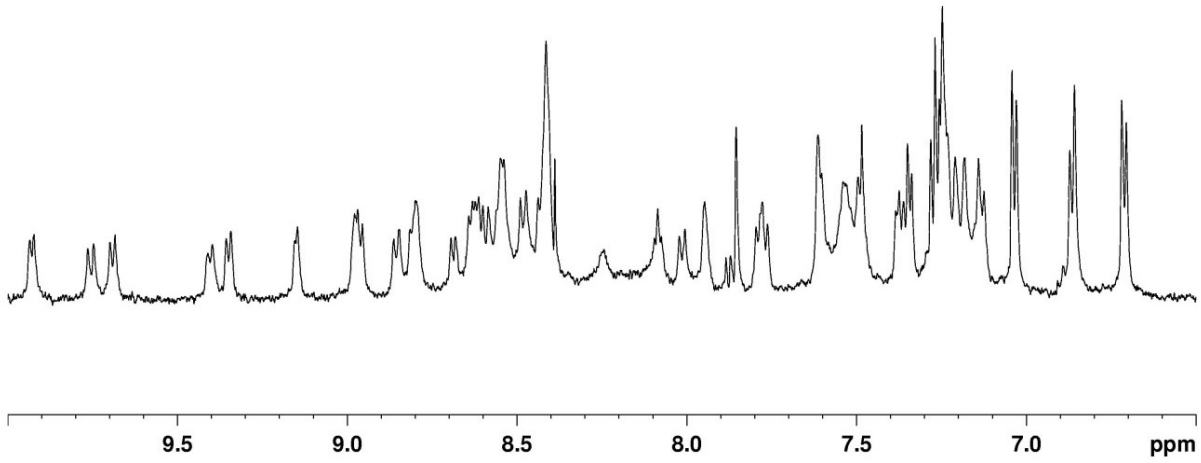


***Figure 5.*** 1D $^{1}$H NMR spectrum of oxidized HBD2 in 20 mM sodium acetate buffer pH 4.0 and 10 % $D_2O$ on a Bruker AVANCE spectrometer equipped with a cryoprobe operating at 600MHz and 25 °C. Only the amide proton region is shown for clarity.

***Antimicrobial and chemotactic activity of recombinant HBD2***

Fully oxidised HBD2 was dissolved in 0.01% acetic acid and the sample was concentrated to 500 μg/mL for the assay. We analysed the activity of the fully oxidised HBD2 against *E. coli* K-12 MG1655, *P. aeruginosa* PAO1, *S. aureus* ATCC 25923 and *C. albicans* J2922 using a previously published assay [25,40,45]. Values of $LD_{50}$, $LD_{90}$ and $MBC_{99.99}$ values against 1 x $10^5$ cells were determined (Table 2). HBD2 was found to be effective in killing Gram-negative bacteria (*E. coli* and *P. aeruginosa*) and yeast *C. albicans* in the μM range, but showed a lower bactericidal effect toward Gram-positive *S. aureus*. These results are in good agreement with that of the natural sample[23], the recombinant HBD2 preparations from other groups [29,46] and peptide prepared by solid-phase peptide synthesis [47] (Table 2).

Yang and colleagues discovered that many defensins are potent chemotactic agents against a range of cells from the mammalian immune system including dendritic cells and T cells [26]. The exact nature of the molecular interactions between HBD2 and the CCR6 receptor are presently unknown but a recent analysis of HBD1/CCR6 has begun to explore the residues involved [22]. It was shown that HBD2 was active in

chemotaxis assays against CCR6, a GPCR previously been shown to be activated by the chemokine CCL20 (MIP3-α). We tested our recombinant HBD2 against HEK293 cells expressing CCR6 in an assay we have used in our laboratory [25] and found that it had optimal activity at 100 ng/ml (Figure 6).

***Table 2.*** Comparison of antimicrobial activity of HBD2 with previous studies (values are in μg/mL, PMB: Polymyxin B as control AMP).

| Strain | Source | $MBC_{99.99}$[a]/MIC[b] | LD90[c] | LD50[d] |
|---|---|---|---|---|
| *E. coli* K12-MG1655 | **This paper** | $MBC_{99.99}$**<20** [a] **(<1.5** [a]**, PMB)** | **3-6** | **<1.5** |
| *E. coli* ML-35 | 47 | 17 [b] | | |
| *E. coli* | 23 | | ~10 | |
| *E. coli* ML35p | 29 | | 4.25-12.25 [f] | |
| *P. aeruginosa* PAO1 | **This paper** | **<25** [a] **(<1.5** [a]**, PMB)** | **<3** | **<1.5** |
| *P. aeruginosa* ATCC 27853 | 47 | 17 [b] | | |
| *P. aeruginosa* | 23 | | ~10 | |
| *P. aeruginosa* ATCC 9027 | 29 | | 4.25-12.25 [f] | |
| *C. albicans* J2922 | **This paper** | **>50** [a] **(<3** [a]**, PMB)** | **>6** | **>1.5** |
| *C. albicans* | 47 | 70 [b] | | |
| *C. albicans* | 23 | | 25 | |
| *C. albicans* 820 | 29 | | 4.25-12.25 [f] | |
| *S. aureus* ATCC 25923 | **This paper** | **>50** [a] **(6** [a]**, PMB)** | **>12** | **>3** |
| *S. aureus* 710A | 47 | 35-70 [b] | | |
| *S. aureus* | 23 | 100 [e] | | |
| *S. aureus* ATCC 6341 | 29 | N.D. [e] | | |

[a] $MBC_{99.99}$ values are the minimum concentration of peptide required to kill 99.99% of initial inoculum.

[b] MIC values are the lowest concentration of peptide that will inhibit the visible growth of a microorganism.

[c] LD90 values are the concentration of peptide required to kill 90% of initial inoculum.

[d] LD50 values are the concentration required to kill 50% of initial inoculum.

[e] Bacteriostatic effect.

[f] Bactericidal effect.

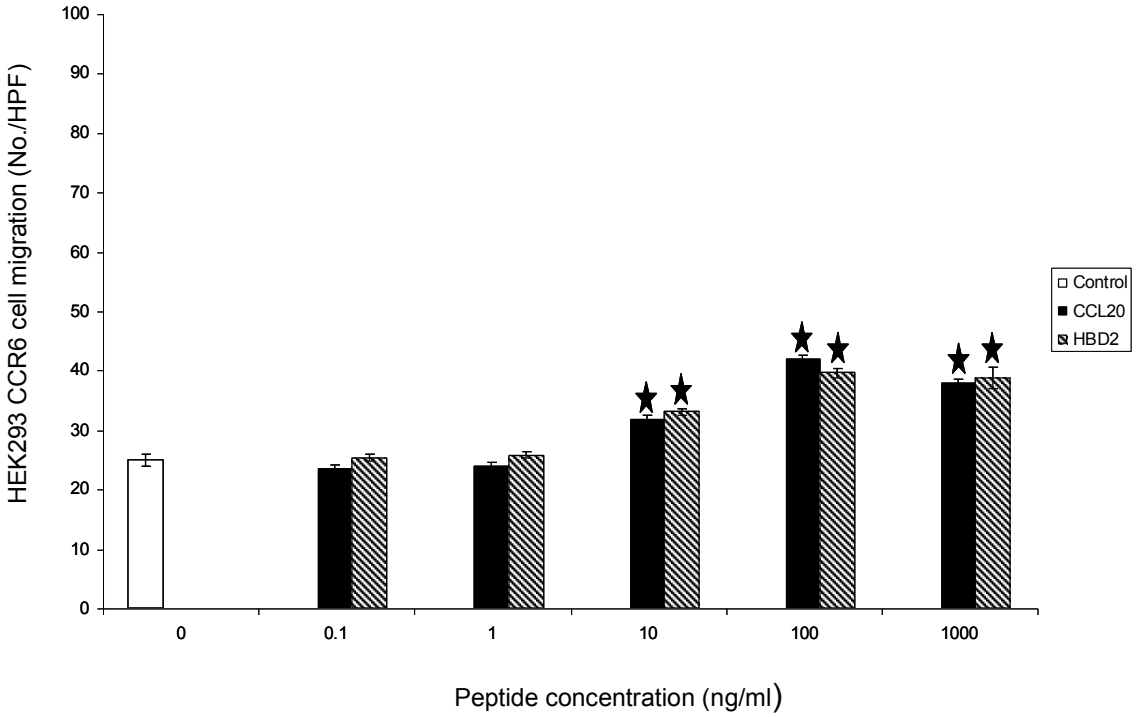


***Figure 6.*** Chemotactic activity of HBD2. The graph shows the number of HEK293 cells expressing the human chemokine receptor CCR6 that migrate towards the peptides. The number of cells per high power field (No./HPF) under the microscope is given. Chemotaxis medium is the control, CCL20 (also known as MIP-3α) is the known chemokine ligand of CCR6. Each assay was repeated three times, numerical data are means ± S.D. and columns with an asterisk indicate peptide with significant activity ($p$<0.05) above culture medium.

## Conclusion

The method described in this paper is straight forward and low-cost, allowing for the production of milligram amounts of β-defensin HBD2 in a commonly-used *E. coli* host. The mature form of HBD2 was isolated as a single, homogenous, oxidized isoform with β-defensin S-S bond connectivity. This HBD2 was an active chemokine for cells expressing the GPCR receptor CCR6 and a potent antimicrobial peptide against a range of microbes. It displayed excellent structural properties (NMR spectroscopy and high resolution mass spectrometry) and is suitable for future analysis of HBD2 in complex with a range of biological targets. The expression clone is also su itable for generation of a range of mutant defensins.

**References**


[1] Zasloff, M. Antimicrobial peptides of multicellular organisms. *Nature,* **2002,** *415*, 389-395.

[2] Crovella, S.; Antcheva, N.; Zelezetsky, I.; Boniotto, M.; Pacor, S.; Verga Falzacappa, M.V. Tossi, A. Primate beta-defensins--structure, function and evolution. *Curr. Protein Pept. Sci.,* **2005,** *6*, 7-21.

[3] Ganz, T. Defensins: antimicrobial peptides of innate immunity. *Nat. Rev. Immunol.,* **2003,** *3*, 710-720.

[4] Lehrer, R.I. Primate defensins. *Nat. Rev. Microbiol.,* **2004,** *2*, 727-738.

[5] Pazgier, M.; Hoover, D.M.; Yang, D.; Lu, W. Lubkowski, J. Human beta-defensins. *Cell. Mol. Life Sci.,* **2006,** *63*, 1294-1313.

[6] Selsted, M.E. Ouellette, A.J. Mammalian defensins in the antimicrobial immune response. *Nat. Immunol.,* **2005,** *6*, 551-557.

[7] Ganz, T.; Selsted, M.E.; Szklarek, D.; Harwig, S.S.L.; Daher, K.; Bainton, D.F. Lehrer, R.I. Defensins. Natural peptide antibiotics of human neutrophils. *J. Clin. Invest.,* **1985,** *76*, 1427-1435.

[8] Schutte, B.C.; Mitros, J.P.; Bartlett, J.A.; Walters, J.D.; Jia, H.P.; Welsh, M.J.; Casavant, T.L. McCray, P.B., Jr. Discovery of five conserved beta -defensin gene clusters using a computational search strategy. *Proc. Natl Acad. Sci. USA,* **2002,** *99*, 2129-2133.

[9] Patil, A.; Hughes, A.L. Zhang, G. Rapid evolution and diversification of mammalian α-defensins as revealed by comparative analysis of rodent and primate genes. *Physiol. Genomics,* **2004,** *20*, 1-11.

[10] de Leeuw, E.; Burks, S.R.; Li, X.; Kao, J.P.Y. Lu, W. Structure-dependent functional properties of human defensin 5. *FEBS Letters,* **2007,** *581*, 515-520.

[11] Lehrer, R.I.; Selsted, M.E.; Szklarek, D. Fleischmann, J. Antibacterial activity of microbicidal cationic proteins 1 and 2, natural peptide antibiotics of rabbit lung macrophages. *Infect. and Immun.,* **1983,** *42*, 10-14.

[12] Szyk, A.; Wu, Z.; Tucker, K.; Yang, D.; Lu, W. Lubkowski, J. Crystal structures of human a-defensins HNP4, HD5, and HD6. *Protein Sci.,* **2006,** *15*, 2749-2760.

[13] Wu, Z.; Ericksen, B.; Tucker, K.; Lubkowski, J. Lu, W. Synthesis and characterization of human α-defensins 4-6. *J. Peptide Res.,* **2004,** *64*, 118-125.

[14] Yang, D.; Chen, Q.; Chertov, O. Oppenheim, J.J. Human neutrophil defensins selectively chemoattract naive T and immature dendritic cells. *J. Leukoc. Biol.,* **2000,** *68*, 9-14.

[15] Bauer, F.; Schweimer, K.; Kluver, E.; Conejo-Garcia, J.R.; Forssmann, W.G.; Rosch, P.; Adermann, K. Sticht, H. Structure determination of human and murine beta-defensins reveals structural conservation in the absence of significant sequence similarity. *Protein Sci.,* **2001,** *10*, 2470-2479.

[16] Hoover, D.M.; Chertov, O. Lubkowski, J. The structure of human beta-defensin-1: new insights into structural properties of beta-defensins. *J. Biol. Chem.,* **2001,** *276*, 39021-39026.

[17] Hoover, D.M.; Rajashankar, K.R.; Blumenthal, R.; Puri, A.; Oppenheim, J.J.; Chertov, O. Lubkowski, J. The structure of human beta-defensin-2 shows evidence of higher order oligomerization. *J. Biol. Chem.,* **2000,** *275*, 32911-32918.

[18] Landon, C.; Thouzeau, C.; Labbe, H.; Bulet, P. Vovelle, F. Solution structure of spheniscin, a beta-defensin from the penguin stomach. *J. Biol. Chem.,* **2004,** *279*, 30433-30439.

[19] Sawai, M.V.; Jia, H.P.; Liu, L.; Aseyev, V.; Wiencek, J.M.; McCray, P.B., Jr.; Ganz, T.; Kearney, W.R. Tack, B.F. The NMR structure of human beta-defensin-2 reveals a novel alpha-helical segment. *Biochemistry,* **2001,** *40*, 3810-3816.

[20] Schibli, D.J.; Hunter, H.N.; Aseyev, V.; Starner, T.D.; Wiencek, J.M.; McCray, P.B., Jr.; Tack, B.F. Vogel, H.J. The solution structures of the human beta-defensins lead to a better understanding of the potent bactericidal activity of HBD3 against Staphylococcus aureus. *J. Biol. Chem.,* **2002,** *277*, 8279-8289.

[21] Zimmermann, G.R.; Legault, P.; Selsted, M.E. Pardi, A. Solution structure of bovine neutrophil beta-defensin-12: the peptide fold of the beta-defensins is identical to that of the classical defensins. *Biochemistry,* **1995,** *34*, 13663-13671.

[22] Pazgier, M.; Prahl, A.; Hoover, D.M. Lubkowski, J. Studies of the biological properties of human β-defensin 1. *J. Biol. Chem.,* **2007,** *282*, 1819-1829.

[23] Harder, J.; Bartels, J.; Christophers, J. Schroder, J.M. A peptide antibiotic from human skin. *Nature,* **1997,** *387*, 861.

[24] Shai, Y. Mode of action of membrane active antimicrobial peptides. *Biopolymers,* **2002,** *66*, 236-248.

[25] Taylor, K.; Clarke, D.J.; McCullough, B.; Chin, W.; Seo, E.; Yand, D.; Oppenheim, J.J.; Uhrin, D.; Govan, J.R.W.; Campopiano, D.J.; MacMillan, D.; Barran, P. Dorin, J.R. Analysis and separation of residues important for the chemoattractant and antimicrobial activities of beta-defensin 3. *J. Biol. Chem.,* **2008,** *283*, 6631-6639.

[26] Yang, D.; Chertov, O.; Bykovskaia, S.; Chen, Q.; Buffo, M.; Shogan, J.; Anderson, M.; Schroder, J.; Wang, J.; Howard, O. Oppenheim, J. Beta-defensins: linking innate and adaptive immunity through dendritic and T cell CCR6. *Science,* **1999,** *286*, 525-528.

[27] Raj, P.A.; Antonyraj, K.J. Karunakaran, T. Large-scale synthesis and functional elements for the antimicrobial activity of defensins. *Biochem. J.,* **2000,** *347 Pt 3*, 633-641.

[28] Kluver, E.; Adermann, K. Schulz, A. Synthesis and structure-activity relationship of β-defensins, multi-functional peptides of the immune system. *J. Pept. Sci.,* **2006,** *12*, 243-257.

[29] Liu, A.Y.; Destoumieux, D.; Wong, A.; Park, C.H.; Valore, E.V.; Liu, L. Ganz, T. Human β-defensin-2 production in keratinocytes is regulated by interleukin-1, bacteria, and the state of differentiation. *J. Invest. Dermatol.,* **2002,** *118*, 275-281.

[30] Porter, E.M.; van Dam, E.; Valore, E.V. Ganz, T. Broad-spectrum antimicrobial activity of human intestinal defensin 5. *Infect. and Immun.,* **1997,** *65*, 2396-2401.

[31] Valore, E.V.; Martin, E.; Harwig, S.S. Ganz, T. Intramolecular inhibition of human defensin HNP-1 by its propiece. *J. Clin. Invest.,* **1996,** *97*, 1624-1629.

[32] Valore, E.V.; Park, C.H.; Quayle, A.J.; Wiles, K.R.; McCray Jr., P.B. Ganz, T. Human β-Defensin-1: an antimicrobial peptide of urogenital tissues. *J. Clin. Invest.,* **1998,** *101*, 1633-1642.

[33] Fang, X.; Peng, L.; Xu, Z.; Wu, J. Cen, P. Cloning and expression of human beta-defensin-2 gene in *Escherichia coli*. *Protein Pept. Lett.,* **2002,** *9*, 31-37.

[34] Pazgier, M. Lubkowski, J. Expression and purification of recombinant human α-defensins in *Escherichia coli*. *Protein Expr. Purif.,* **2006,** *49*, 1-8.

[35] Xu, Z.; Peng, L.; Zhong, Z.; Fang, X. Cen, P. High-level expression of a soluble functional antimicrobial peptide, human beta-defensin 2, in Escherichia coli. *Biotechnol. Prog.,* **2006,** *22*, 382-386.

[36] Zhong, Z.; Xu, Z.; Peng, L.; Huang, L.; Fang, X. Cen, P. Tandem repeat mhBD2 gene enhance the soluble fusion expression of hBD2 in Escherichia coli. *Appl. Microbiol. Biotechnol.,* **2006,** *71*, 661-667.

[37] Chen, H.; Xu, Z.; Xu, N. Cen, P. Efficient production of a soluble fusion protein containing human beta-defensin-2 in *E. coli* cell-free system. *J. Biotechnol.,* **2005,** *115*, 307-315.

[38] Cipakova, I. Hostinova, E. Production of the human-beta-defensin using *Saccharomyces cerevisiae* as a host. *Protein Pept. Lett.,* **2005,** *12*, 551-554.

[39] Boniotto, M.; Antcheva, N.; Zelezetsky, I.; Tossi, A.; Palumbo, V.; Verga Falzacappa, M.V.; Sgubin, S.; Braida, L.; Amoroso, A. Crovella, S. A study of host defence peptide β-defensin 3 in primates. *Biochem. J.,* **2003,** *374*, 707-714.

[40] Campopiano, D.J.; Clarke, D.J.; Polfer, N.C.; Barran, P.E.; Langley, R.J.; Govan, J.R.; Maxwell, A. Dorin, J.R. Structure-activity relationships in defensin dimers: a novel link between beta-defensin tertiary structure and antimicrobial activity. *J. Biol. Chem.,* **2004,** *279*, 48671-48679.

[41] Clarke, D.J. Campopiano, D.J. Structural and functional studies of defensin-inspired peptides. *Biochem. Soc. Trans.,* **2006,** *34*, 251-256.

[42] Maemoto, A.; Qu, X.; J., R.K.; Tanabe, H.; Henschen-Edman, A.; Craik, D.J. Ouellette, A.J. Functional analysis of the α-defensin disulfide array in mouse cryptdin-4. *J. Biol. Chem.,* **2004,** *279*, 44188-44196.

[43] Stemmer, W.P.; Crameri, A.; Ha, K.D.; Brennan, T.M. Heyneker, H.L. Single-step assembly of a gene and entire plasmid from large numbers of oligodeoxyribonucleotides. *Gene,* **1995,** *164*, 49-53.

[44] Wu, Z.; Hoover, D.M.; Yang, D.; Boulegue, C.; Santamaria, F.; Oppenheim, J.J.; Lubkowski, J. Lu, W. Engineering disulfide bridges to dissect antimicrobial and chemotactic activities of human beta-defensin 3. *Proc. Natl Acad. Sci. USA,* **2003,** *100*, 8880-8885.

[45] Taylor, K.; McCullough, B.; Clarke, D.J.; Langley, R.J.; Pechenick, T.; Hill, A.; Campopiano, D.J.; Barran, P.E.; Dorin, J.R. Govan, J.R. Covalent dimer species of beta-defensin Defr1 display potent antimicrobial activity against multidrug-resistant bacterial pathogens. *Antimicrobiol. Agents. Chemother.,* **2007,** *51*, 1719-1724.

[46] Feng, Z.; Jiang, B.; Chandra, J.; Ghannoum, M.; Nelson, S. Weinberg, A. Human beta-defensins: differential activity against candidal species and regulation by *Candida albicans*. *J. Dent. Res.,* **2005,** *84*, 445-450.

[47] Antcheva, N.; Boniotto, M.; Zelezetsky, I.; Pacor, S.; Verga Falzacappa, M.V.; Crovella, S. Tossi, A. Effects of positively selected sequence variations in human and *Macaca fascicularis* beta-defensins 2 on antimicrobial activity. *Antimicrob. Agents Chemother.,* **2004,** *48*, 685-688.